Abdominal Radiology

Published online: 28 August 2018

Abdom Radiol (2019) 44:568–575
https://doi.org/10.1007/s00261-018-1754-2

Lower energy levels and iodine-based material decomposition images increase pancreatic ductal adenocarcinoma conspicuity on rapid kV-switching dual-energy CT

Serdar Aslan,[1] Ilkay Camlidag,[2] and Mehmet Selim Nural[2]

[1]Radiology Clinic, Turhal State Hospital, 60300 Tokat, Turkey
[2]Department of Radiology, Faculty of Medicine, Ondokuz Mayis University, Samsun, Turkey

Abstract

Purpose: Multidetector computed tomography (MDCT) is used in the diagnosis of pancreatic ductal adenocarcinoma (PDAC), but it may be inadequate in some cases. Tumor detection can be improved using rapid kV-switching dual-energy CT (rsDECT) and iodine maps. Our aim this study is to evaluate tumor conspicuity in PDAC cases using rsDECT and iodine maps.

Methods: Ninety cases with PDAC were evaluated rsDECT. Tumor contrast (HU) differences, tumor size, CNR (contrast-noise ratio), and noise were measured at 70 keV, individual CNR-energy level, and 45 keV, respectively. Quantitative differences in contrast gain Δ70-CNR and ΔCNR-45 were compared. On iodine maps, the iodine concentration measured in the tumor and parenchyma was normalized to the aorta as normalized iodine concentration (NIC) and compared.

Results: The median optimized viewing energy level was 51 keV. The mean ± SD tumor contrast values were 62 ± 20, 115 ± 48, and 152 ± 48 HU ($p < 0.001$); the largest axial diameters were 36.6 ± 5.1, 37.9 ± 4.2, and 38.3 ± 3.7 mm ($p = 0.015$); the CNRs were 1.83 ± 0.72, 3.37 ± 0.93, and 2.36 ± 0.56; and the image noise levels were 23.7 ± 6.8, 39.3 ± 11.6, and 59.5 ± 17.2 ($p < 0.001$) ($p < 0.001$) for 70 keV, optimized energy level, and 45 keV, respectively. The mean ± SD contrast gain Δ70-CNR was 63 ± 12; and ΔCNR-45 was 31 ± 26 HU ($p < 0.001$). NIC_{tumor} and $NIC_{parenchyma}$ values were 0.62 ± 0.03 and 1.36 ± 0.05 mg/mL, respectively ($p = 0.004$).

Conclusion: The use of low energy levels on rsDECT and iodine maps improves tumor conspicuity. This situation may be help better detection of pancreatic tumors.

Key words: Pancreatic ductal adenocarcinoma—Rapid kV-switching dual-energy computed tomography—İodine concentration

Pancreatic ductal adenocarcinoma (PDAC) continues to be a destructive diagnosis and is expected to become the second leading cause of cancer mortality by 2030 [1, 2]. Early diagnosis is very important because the 5-year survival rate can be improved with surgery or adjuvant intervention. Imaging methods play a very important role in diagnosis. The most commonly used imaging method is multidetector computed tomography (MDCT) [3–5]. Other imaging modalities such as endoscopic ultrasonography (EUS) and magnetic resonance imaging are also used for diagnosis and to guide decisions on surgical resection.

Pancreatic ductal adenocarcinoma (PDAC) shows intense fibrosis and is often seen on MDCT as hypoattenuating compared with parenchyma, so it is best detected on pancreatic parenchymal phase images [6]. Recent retrospective studies have reported that MDCT may help a PDAC diagnosis be made a few months before clinical diagnosis [3, 7]. However, 11%–27% of PDACs are seen as isoattenuating compared with adjacent parenchyma on MDCT, and this makes diagnosis difficult [4, 8, 9]. MDCT may be insufficient to detect small-sized isoattenuating tumors. Rapid kV-switching dual-energy CT (rsDECT) pancreatic parenchymal phase images can detect hypoattenuating tumors at low energy levels, show tumor size more accurately, and reduce the number of 'undetectable' early-stage lesions and isoat-

Correspondence to: Serdar Aslan; *email:* serdaraslan28@hotmail.com

tenuating tumors [7]. Accordingly, using monochromatic images obtained with rsDECT increases PDAC detection.

Today, three different DECT technologies (rsDECT, dual-source dual-energy (DSDE), and dual-layer spectral imaging) on the market produce information at different levels of photon energies, using differences in material composition and therefore differences in the absorption and attenuation of photons. The increase of photon energy causes a decrease in the photoelectric effect and an increase in Compton scattering. Thus, attenuation in iodine density is more pronounced at lower energy levels than at higher energy levels [10–13]. Hypoattenuating pancreatic tumors on pancreatic parenchymal phase images are better selected at low energy levels than at high energy levels for all DECT technologies. The only disadvantage of lower energy levels is increased image noise [14].

rsDECT uses a single X-ray source that changes keV value at submillisecond intervals between 40 and 140 keV. The images obtained from the 70 keV image series are similar to the MDCT images obtained with the standard 120 kVp. This modality allows the obtained data to be reprocessed in X-ray projections to generate a monochromatic imaging series simulated with 1 keV increments from 40 to 140 keV. It also allows spectral evaluation and determination of the contrast-to-noise ratio (CNR)—optimized energy level on an independent workstation. Iodine-based material decomposition images (iodine maps) and virtual monochromatic images can also be obtained from rsDECT images with the aid of workstations. With the help of iodine maps, quantitative iodine quantities of lesions can be calculated. This suggests that iodine maps may be useful in detecting isoattenuating PDACs [15].

Our aim in this study is to evaluate changes in the contrast of PDACs using rsDECT images utilizing three energy levels: 70 keV, individual CNR-optimized viewing energy level, and 45 keV; and to determine the effect of iodine maps on tumor detectability.

Materials and methods

This prospective study was approved by our institutional ethics committee. Informed consent was obtained from all individual participants included in the study.

Study population

This study was carried out between June 2016 and August 2017. A hundred and twenty-three cases who were scheduled for biphasic pancreatic protocol MDCT examination with a presumed diagnosis of pancreatic tumor were eligible for the study. Exclusion criteria were presence of any renal function disorder, a known allergy to contrast medium (CM), history of pancreatic surgery or chemotherapy, absence of a pathological diagnosis (n = 20) or diagnoses other than PDAC like MFCP, endocrine tumors, and other cystic and solid masses (n = 13). Patients with a definite histopathological diagnosis of PDAC by surgery (n = 25), percutaneous biopsy (n = 17), or endoscopic ultrasound (EUS)-guided fine needle aspiration cytology (FNAC) (n = 48) were included in the study. Inclusion and exclusion criteria for the study and the MDCT imaging features of the patients included in the study are presented in flow diagram (Fig. 1).

Imaging protocol

The patients were examined while supine using a biphasic pancreatic protocol with 64-slice rsDECT (Discovery CT750 HD, GE Healthcare, Milwaukee, WI). Vascular access from an antecubital vein was achieved with an 18-gauge cannula. With the help of a power injector (Ulrich Inject CT Motion, Synapse Medical, Dublin, Ireland), 80–100 mL of non-ionic contrast medium (Iopamidol: Isovue 370; Bracco, Milan, Italy) with 0.5 g of iodine per kilogram of body weight was administered at a rate of 4 mL/s.

The trigger threshold method was used during the scan to minimize hemodynamic differences. The aortic region of interest (ROI) was placed at the supraceliac level, and the density was measured. Pancreatic parenchymal phase images were taken 20 s after the value of density reached 80 HU. Portal venous phase images were taken after 50 s. Pancreatic parenchymal phase images were obtained using a dual-energy technique, and portal venous phase images were obtained using a conventional MDCT technique. All images were obtained as 0.625 mm.

Total dose-length product (DLP) for all phases, for the pancreatic parenchymal phase acquired in dual-energy, and for the portal venous phase were recorded for each patient. The formula DLP × conversion factor (0.015) was used for effective dose calculation.

Image analysis

All 90 patients were evaluated with a Gemstone Spectral Viewer (GSI, AW Server, GE Healthcare) on a scanner-independent workstation. Two board-certificated abdominal radiologists (5 and 12 years of experience, respectively) reviewed the MDCT images, including conventional images, monochromatic images, and iodine maps, with the GSI Viewer in consensus at a workstation. Disagreement on diagnosis was resolved by a third board-certificated abdominal radiologist (12 years of experience). Tumor was determined on MDCT images, and contrast was measured at three energy levels: 70 keV, CNR-optimized energy level, and 45 keV (Fig. 2A–D). If no mass was visible, the radiologists were

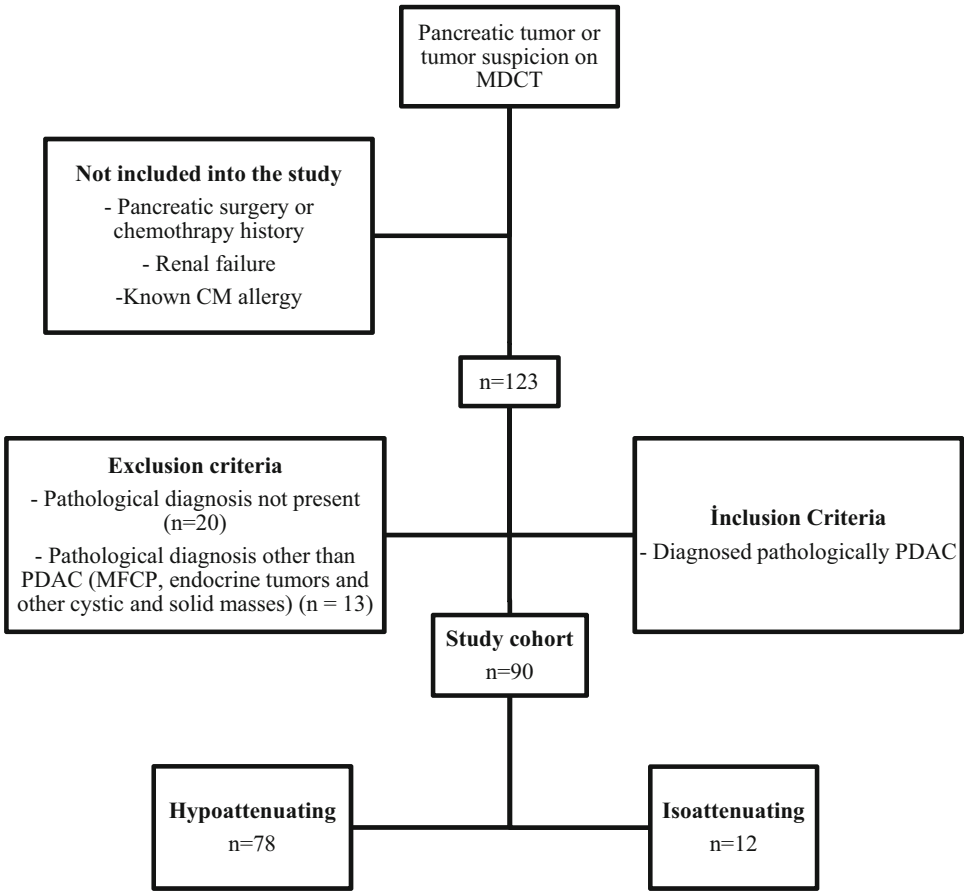

Fig. 1. Flow diagram showing the criteria for inclusion and exclusion and MDCT imaging features of the cases into the study.

instructed to place the "tumor" ROI at the site of the abrupt main pancreatic duct termination or focal irregularity in the contour of the pancreas. The tumor and parenchyma ROIs were placed away from vascular structures, the pancreatic duct, and focal necrosis areas. The ROI setting was performed on the 70 keV images and then propagated to the other two energy levels. Although the lowest energy level allowed by the workstation was 40 keV, we used 45 keV as the lowest energy level because the image noise was very high at 40 keV. The CNR-optimized energy level was calculated by the GSI Viewer using an automated feature after ROIs had been placed at the tumor and parenchyma (Fig. 3A, B). We used the 70 keV image series to calculate the CNR-optimized energy level. At all energy levels, the largest axial diameter of the tumor was recorded.

The quantitative contrast gain (change in radiodensity [HU] difference between tumor and normal parenchyma) for each patient was calculated between 70 keV and the CNR-optimized energy level, abbreviated as Δ70-CNR, as well as between the CNR-optimized energy level and 45 keV, abbreviated as ΔCNR-45. Iodine maps were used to calculate the iodine concentration of the tumor and parenchyma (Fig. 4). The iodine concentration measured in the tumor and parenchyma was normalized to the aorta as normalized iodine concentration (NIC) to minimize variations in scan time and iodine concentration between cases ($NIC_{tumor} = IC_{tumor}/IC_{aorta}$ and $NIC_{parenchyma} = IC_{parenchyma}/IC_{aorta}$).

Tumors seen as isoattenuating and hypoattenuating on pancreatic phase images were defined as subgroups. Isoattenuating tumors were defined as those with a 10–15 HU attenuation difference compared with adjacent parenchyma. If no mass was visible, the tumor was considered to be the site of the abrupt main pancreatic duct termination or focal irregularity in the contour of the pancreas. Hypoattenuating tumors were visually hypoattenuation compared with the parenchyma.

Noise was documented using the standard deviation of an ROI placed in the left paraspinal muscles of the upper abdomen in each patient, using a uniform 1.5 mm^2 oval at identical locations for the same three energy levels. CNRs were calculated for each patient at each energy level using the following equation: attenuation of normal parenchyma—tumor/SD of paraspinal muscle.

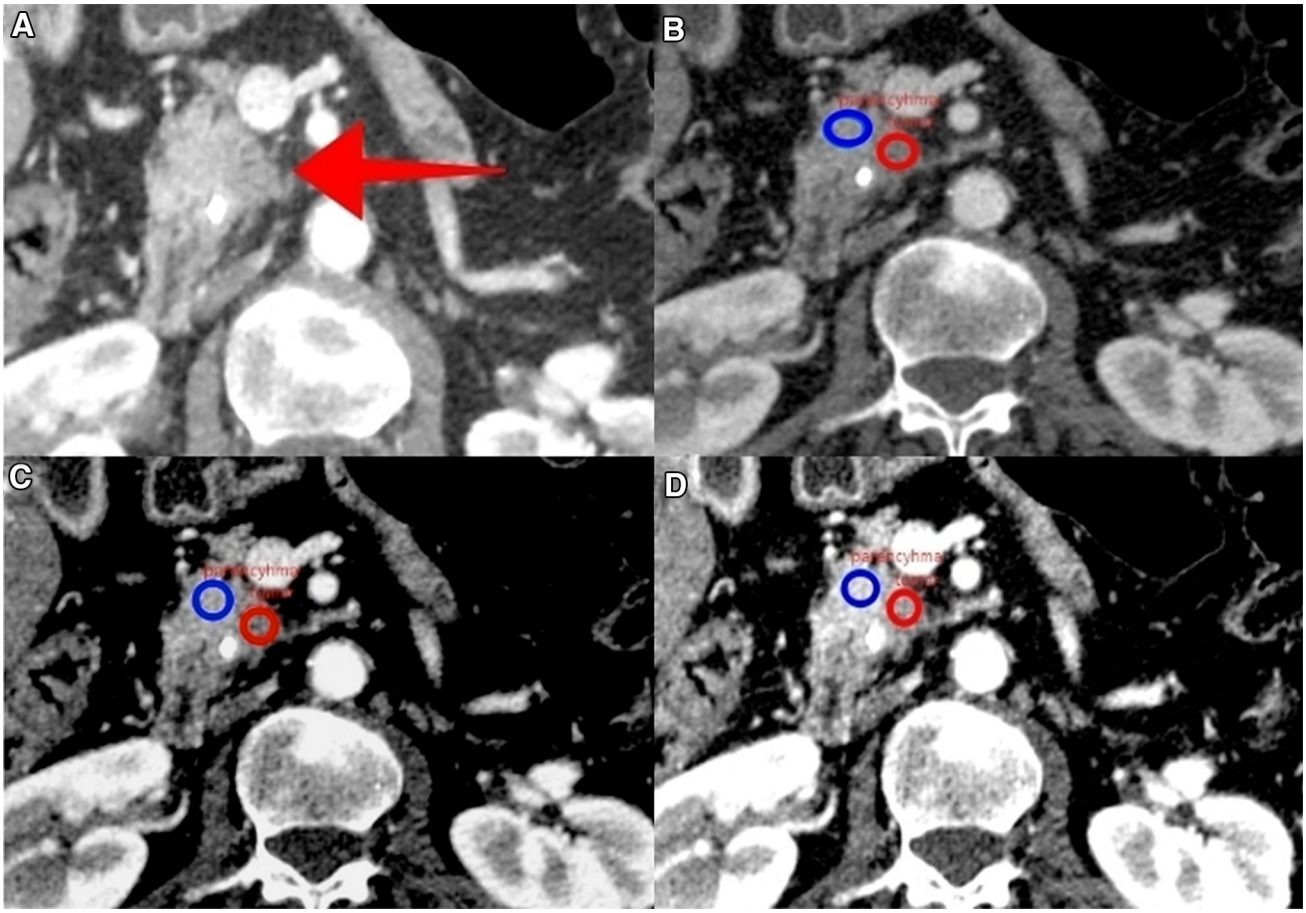

Fig. 2. A 63-year-old woman with resectable pancreatic ductal adenocarcinoma in the head of the pancreas. Blue and red circles represent the radiodensity measurements of the normal pancreas and the tumor, respectively. **A** Standard pancreatic phase MDCT image (120 kVp) reveals a small isoattenuating mass in the pancreas head which cannot be distinguished from the normal parenchyma (red arrow). A plastic biliary stent is in place. **B** A 70 keV Gemstone Spectral Image (GSI) at 0.625 mm at the same level. Normal pancreas radiodensity is 152 HU and tumor radiodensity is 93 HU. Tumor contrast is 59 HU. **C** CNR-optimized image at 53 keV. Normal pancreas radiodensity is 269 HU and tumor radiodensity is 157 HU. Tumor contrast is 112 HU. **D** Image at 45 keV. Normal pancreas radiodensity is 365 HU and tumor radiodensity is 228 HU. The tumor contrast is 137 HU. As the energy level decreases, the difference in radiodensity between the normal pancreas and the tumor appears to increase. However, the tumor is best viewed at the CNR-optimized viewing energy level. Surgical pathology results revealed a 2.5 cm moderately differentiated adenocarcinoma.

Statistical analysis

Statistical analyses were done with SPSS software, version 21 (IBM Corporation, Armonk, NY, USA). All parameters were expressed as mean ± standard deviation. Tumor contrast [normal parenchyma density (HU) − tumor density (HU)], the largest axial tumor diameter, CNR, and image noise at different keV values were compared using analysis of variance test (ANOVA). The parameters of the cases with hypoattenuating and isoattenuating tumors, quantitative changes in contrast gain between the energy levels for a given subject (△70-CNR and 45-△CNR), and NIC (NIC_{tumor} and $NIC_{parenchyma}$) were compared using the Student *t* test. A *p* value less than 0.05 was considered statistically significant.

Results

Study population

Ninety patients [43 women, 47 men; mean age, 71 ± 11.8 years (± SD); range 48–94 years] were finally included in the study. Eighteen patients (20%) had resectable disease, 7 (7.7%) had borderline resectable disease, 38 (42.2%) had local advanced pancreatic cancer, and 37 (41.1%) had distant metastasis.

Image analysis

Comparison of different monochromatic energy level measurements of hypoattenuating and isoattenuating

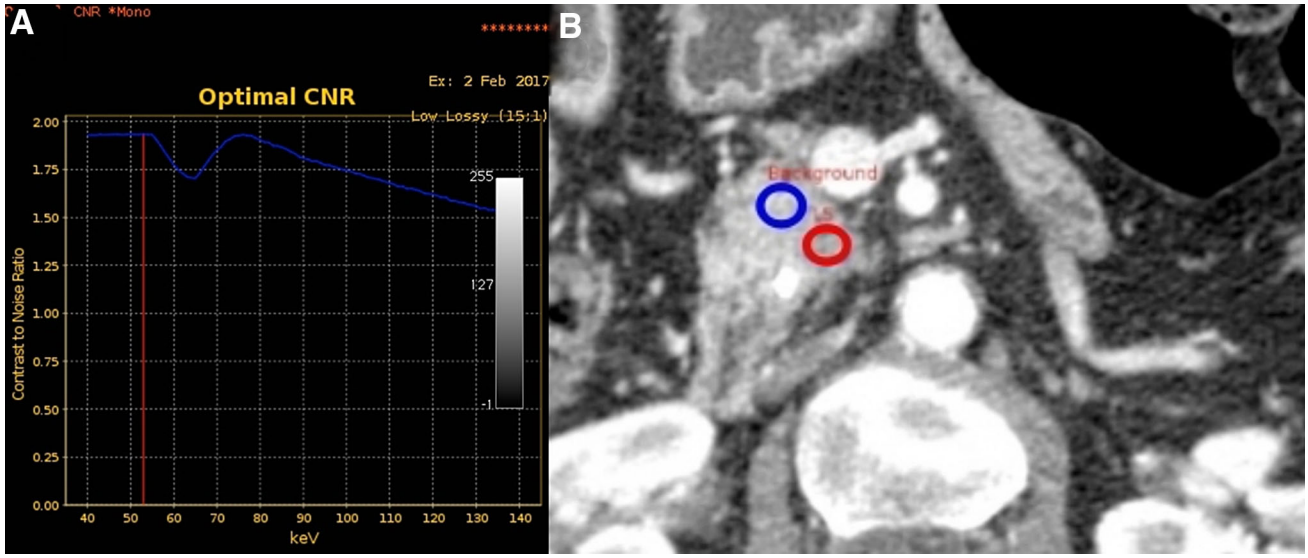

Fig. 3. Same case as given in Fig. 2, demonstrating the GSI Viewer calculation of the CNR curve on (53 keV) (**A**) and the locations of the background normal parenchyma (blue circle) and tumor (red oval) ROIs to generate the curve on (**B**).

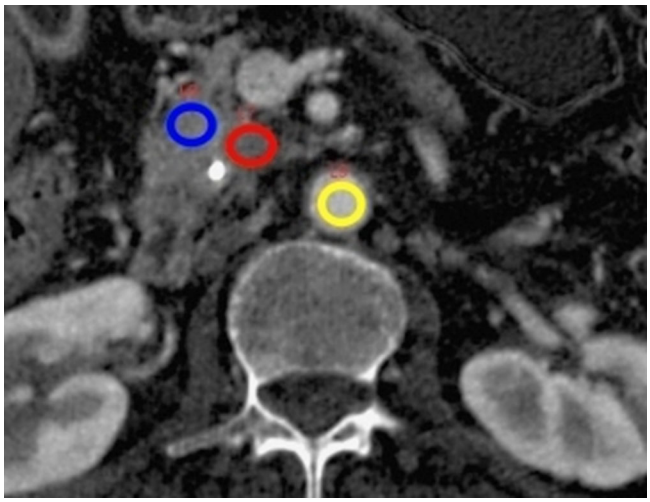

Fig. 4. On iodine-based material decomposition images, the aorta (yellow circle), normal parenchyma (blue circle), and tumor (red circle) ROIs were placed to calculate normalized iodine concentration (NIC).

tumors is provied in Table 1. The tumor was hypoattenuating in 78 patients (86.7%) and isoattenuating in 12 patients (13.3%) compared with normal parenchyma. For all patients, the CNR-optimized viewing energy level (mean ± SD) was calculated 52 ± 8.5 keV (range 40–73 keV). We found no significant difference among the compared measurements of hypoattenuating and isoattenuating tumors except for CNR at 70 keV ($p = 0.022$) and CNR at CNR-optimized viewing energy ($p = 0.014$). For all three image-viewing energy levels, the absolute monochromatic density values for both the tumor and normal parenchyma generally increased as the energy levels decreased, as did the lesion contrast as defined as the difference between the values.

For all patients, the tumor contrast values at 45 keV (152 ± 48 HU) were significantly higher than the tumor contrast values at 70 keV and CNR-optimized keV (62 ± 20 and 115 ± 48 HU, respectively; $p < 0.001$). The largest axial diameter (LAD) at 45 keV was significantly higher (38.3 ± 2.7 mm) than the axial diameter measured at 70 keV and CNR-optimized keV (36.6 ± 5.1 and 37.9 ± 4.2 mm, respectively; $p = 0.015$). The CNR at CNR-optimized energy level (3.37 ± 0.93) was significantly higher than the CNR at 45 and 70 keV (2.36 ± 0.56 and 1.83 ± 0.72, respectively; $p < 0.001$). The image noise at 45 keV (59.5 ± 17.2) was significantly higher than the image noise at 70 keV and CNR-optimized keV (23.7 ± 6.8 and 39.3 ± 11.6, respectively; $p < 0.001$). For individual patients, the quantitative contrast gain attenuation increase at △70-CNR was significantly higher than the contrast gain attenuation at △CNR-45 (63 ± 12 vs. 31 ± 26 HU; $p < 0.001$). The NIC_{tumor} value was significantly lower than the $NIC_{parenchyma}$ value (0.62 ± 0.03 vs 1.36 ± 0.05 mg/mL; $p = 0.004$).

For 12 isoattenuating tumors separated as subgroup, the CNR-optimized viewing energy level (mean ± SD) was calculated 52 ± 6.2 keV (range 47-63 keV). For isoattenuating tumors, the tumor contrast values at 45 keV (147 ± 38 HU) were significantly higher than the tumor contrast at 70 keV and CNR-optimized keV (66 ± 16 and 111 ± 51 HU, respectively; $p = 0.004$). The LAD at 45 keV was significantly higher (36.6 ± 4.1 mm) than the axial diameter measured at 70 keV and CNR-optimized keV (33.9 ± 2.8 and 35.7 ± 3.7 mm, respectively; $p = 0.003$). The CNR at

Table 1. Comparison of hypoattenuating and isoattenuating pancreatic ductal adenocarcinomas with rapid kV-switching dual-energy computed tomography (rsDECT)

	All cases (n = 90)	Hypoattenuating tumors (n = 78)	Isoattenuating tumors (n = 12)	p^a
CNR-optimized viewing energy (keV)	52 ± 8.5	53 ± 7.1	52 ± 6.2	0.586
LAD at 70 keV (mm)	36.6 ± 5.1	37.3 ± 6.3	33.9 ± 2.8	0.325
LAD at CNR-optimized viewing energy (mm)	37.9 ± 4.2	38.6 ± 6.5	35.7 ± 3.7	0.613
LAD at 45 keV (mm)	38.3 ± 2.7	39.2 ± 3.2	36.6 ± 4.1	0.528
Tumor contrast at 70 keV (HU)	62 ± 20	59 ± 16	66 ± 16	0.537
Tumor contrast at CNR-optimized viewing energy (HU)	115 ± 48	117 ± 47	111 ± 51	0.624
Tumor contrast at 45 keV (HU)	152 ± 48	154 ± 42	147 ± 38	0.309
△70-CNR (HU)	63 ± 12	63 ± 10	63 ± 16	0.977
△CNR-45 (HU)	31 ± 26	33 ± 13	22 ± 10	0.79
CNR at 70 keV	1.83 ± 0.72	1.91 ± 0.71	1.3 ± 0.52	**0.022**
CNR at CNR-optimized viewing energy	3.37 ± 0.93	3.42 ± 0.98	3.07 ± 0.32	**0.014**
CNR at 45 keV	2.36 ± 0.56	2.41 ± 0.58	2.03 ± 0.28	0.816
NIC_{tumor} (mg/mL)	0.62 ± 0.03	0.64 ± 0.2	0.5 ± 0.24	0.939
$NIC_{parenchyma}$ (mg/mL)	1.36 ± 0.05	1.4 ± 0.33	0.97 ± 0.11	0.093

Results expressed in mean ± standard deviation
CNR, Contrast-to-noise ratio; NIC, Normalized iodine concentration; HU, Hounsfield Unit
[a] p hypoattenuating tumors vs. isoattenuating tumors
$p < 0.05$ were taken as statistically significant and significant p values have been highlighted in bold

CNR-optimized energy level (3.07 ± 0.32) was significantly higher than the CNR at 45 keV and 70 keV (2.03 ± 0.28 and 1.3 ± 0.52, respectively; $p < 0.001$), similar to other cases. The image noise at 45 keV (58.3 ± 15.2) was significantly higher than the image noise at 70 keV and CNR-optimized keV (24.6 ± 7.2 and 41.3 ± 12.5, respectively; $p < 0.001$). The quantitative contrast gain attenuation increase at △70-CNR was significantly higher than the contrast gain attenuation at △CNR-45 (63 ± 16 vs. 22 ± 10 HU; $p = 0.001$). The NIC_{tumor} value was significantly lower than the $NIC_{parenchyma}$ value (0.5 ± 0.24 vs. 0.97 ± 0.11; $p = 0.004$).

The facts that the highest CNR was obtained at the CNR-optimized energy level and the image noise was lower than the image noise at 45 keV indicate that tumor detectability was increased at the CNR-optimized energy level in all cases.

The DLPs for the entire MDCT examination, the dual-energy pancreatic phase, and the portal venous phase were calculated as 1250 ± 421, 560 ± 88, and 750 ± 102 mGy cm, respectively, using CTDIvol mean 17.8 mGy. The effective radiation doses of the MDCT examination, the dual-energy pancreatic phase, and the portal venous phase were calculated as 16.2 ± 4.1, 8.6 ± 1.3, and 10.9 ± 2.3 mSv, respectively.

Discussion

Our study showed that PDAC contrast was significantly increased at low energy levels of spectral MDCT. The best tumor contrast was obtained at 45 keV in all the images, and this was the lowest value used in the study. However, in all cases, the highest CNR value was found at the CNR-optimized energy level. In all cases, the highest image noise was measured at 45 keV. The contrast gain observed at the CNR-optimized energy level and the relatively low image noise at 45 keV, and monochromatic images obtained at the CNR-optimized energy level produced an increase in tumor detectability.

In the literature, the number of studies evaluating PDAC detectability with DECT is limited. Macari et al. reported that in dual-source dual-energy (DSDE) MDCT studies of 15 patients, tumor detectability at 80 kVp was better than with weighted 120 kVp, and Graser et al. showed that tumor detection with DSDE was better at 80 kVp than at 120 and 140 kVp [10, 11]. The rsDECT study by Patel et al. found that PDAC contrast and detectability increase at low energy levels. In the same study, the authors stated that the images obtained with the CNR-optimized energy level had the potential to increase the tumor's specificity [14]. Our study had the widest group of patients so far in the literature, and our results are similar to findings in the literature.

The rsDECT that we used in our study allowed spectral analysis and determination of the CNR-optimized energy level. However, in DSDE, images obtained with 80 and 140 kVp can be evaluated separately or with weighted 120 kVp images, but spectral analysis and determination of the CNR-optimized energy level are not possible to assess. Spectral analysis allows monochromatic images to show objects that are examined when the X-ray source produces monochromatic X-ray photons. This increases the contrast and the spatial resolution. With this feature, we think that rsDECT has an advantage over DSDE, which scans at low energy levels. Another advantage of rsDECT is that it allows calculation of the CNR-optimized energy level. Thus, the best indi-

vidual energy level can be determined for lesion imaging in each case.

In our study, we calculated NIC_{tumor} and $NIC_{parenchyma}$ values on an iodine map and compared them to each other. In all cases (including isoattenuating tumors), we found that the NIC_{tumor} value was significantly lower than the $NIC_{parenchyma}$ value. Our study is the first in the literature to compare NIC_{tumor} and $NIC_{parenchyma}$ values of PDACs. McNamara et al. found that the tumor iodine concentration was lower than the pancreatic parenchyma iodine concentration [16]. However, those researchers did not calculate NIC values. We believe that NIC values may be useful for the detection of small tumors as well as isodense tumors, as they give quantitative results.

No significant difference was seen in CNR-optimized energy level and tumor contrast gain between hypoattenuating and isoattenuating tumors in our study. We found that isoattenuating tumors were more prominently observed at the CNR-optimized energy level (51 keV) than at 70 keV. We suggest that if the rsDECT technique is used in patients with isoattenuating tumors, an evaluation made with the CNR-optimized energy level will provide contrast gain and will allow the tumor to be identified more clearly.

In our study, we detected the highest image noise at the lowest energy level of 45 keV and the highest CNR at the CNR-optimized energy level. Even if the contrast of the tumor at low energy levels (45 keV) is increased relative to other energy levels examined, the effect of higher contrast on tumor detectability should be controversial. In other words, images obtained with low energy levels (45 keV) increase the contrast difference between tumor and normal parenchyma; however, the high image noise decreases tumor conspicuity.

In our study, small but significant differences were observed in tumor sizes measured at three different energy levels, which may be related to irregularity of the tumor boundaries due to increased noise as energy levels go down or to the tendency of tumor dimensions to be measured as larger because of the increase in tumor contrast at low energy levels. Surgical and pathologically correlated studies may provide more clarity on this subject.

We used the AW workstation to evaluate monochromatic images and iodine maps. The AW workstation uses the GSI Viewer software. The GSI Viewer software package automatically calculated and displayed the CNR values for our 101 sets of monochromatic images in real time. We think that this software program is very useful and sufficient for diagnosis.

As with all CT techniques, there is concern about radiation dose with DECT. In Graser et al.'s study using DSDE, the effective radiation dose was found to be between 4.5 and 12.5 mSv, and in Patel et al.'s study using pancreatic phase size-specific dose estimate, the effective radiation dose was found to be 9.1 ± 1.3 mSv [11, 14]. The average radiation dose in our study was similar to those in the literature.

Our study had some limitations. Firstly, our study is the first rsDECT study to evaluate isoattenuating PDACs, but our patient group was small. Studies with larger groups will help researchers get a clearer perspective. Secondly, the evaluations were made by two radiologists by consensus. When consensus could not be reached, a third radiologist evaluated the images. It was not possible to evaluate interreader compliance. Our results, however, show that the contrast gain between the tumor and normal parenchyma using the CNR-optimized energy level in the literature was similar to that found by Patel et al. and Lu et al. [14, 17].

In conclusion, the use of low energy levels on rsDECT and iodine maps in evaluating PDACs increases tumor detectability. This approach identifies small pancreatic tumors and isoattenuating tumors earlier and more clearly, especially those with poor diagnosis and delayed onset. We believe that in routine clinical use, CNR-optimized energy levels may improve detectability of these tumors without degrading image quality, reducing image quality degradation on images obtained with lower energy levels.

Compliance with ethical standards

Funding No funding was received for this study.

Conflict of interest The authors declare that they have no conflict of interest.

Ethical approval All procedures performed in studies involving human participants were in accordance with the ethical standards of the institutional research committee and the 1964 Declaration of Helsinki and its later amendments or comparable ethical standards. For this type of study formal consent is not required.

References

1. American Cancer Society (2013) *Cancer facts and figures*. Atlanta: American Cancer Society
2. Rahib L, Smith BD, Aizenberg R, et al. (2014) Projecting cancer incidence and deaths to 2030: the unexpected burden of thyroid, liver, and pancreas cancers in the United States. Cancer Res 74:2913–2921
3. Sahani DV, Shah ZK, Catalano OA, Boldan GW, Brugge WR (2008) Radiology of pancreatic adenocarcinoma: current status of imaging. J Gastroenterol Hepatol 23:23–33
4. Klauss M, Stiller W, Pahn G, et al. (2013) Dual-energy perfusion-CT of pancreatic adenocarcinoma. Eur J Radiol 82:208–214
5. Callery MP, Chang KJ, Fishman EK, et al. (2009) Pretreatment assessment of resectable or borderline resectable pancreatic cancer: expert consensus statement. Ann Surg Oncol 16:1727–1733
6. Grözinger G, Grözinger A, Horger M (2014) The role of volume perfusion CT in the diagnosis of pathologies of the pancreas. Fortschr Röntgenstr 186:1082–1093
7. Gangi S, Fletcher JG, Nathan MA, et al. (2004) Time interval between abnormalities seen on CT and the clinical diagnosis of pancreatic cancer: retrospective review of CT scans obtained before diagnosis. Am J Roentgenol 82:897–903

8. Prokesch RW, Chow LC, Beaulieu CF, Bammer R, Jeffrey RB (2002) Isoattenuating pancreatic adenocarcinoma at multi–detector row CT: secondary signs. Radiology 224:764–768
9. Kim JH, Park SH, Yu ES, et al. (2010) Visually isoattenuating pancreatic adenocarcinoma at dynamic-enhanced CT: frequency, clinical and pathologic characteristics, and diagnosis at imaging examinations. Radiology 257:87–96
10. Macari M, Spieler B, Kim D, et al. (2010) Dual-source dual-energy MDCT of pancreatic adenocarcinoma: initial observations with data generated at 80 kVp and at simulated weighted-average 120 kVp. Am J Roentgenol 194:27–32
11. Graser A, Johnson TR, Chandarana H, Macari H (2009) Dual-energy CT: preliminary observations and potential clinical applications in the abdomen. Eur Radiol 19:13–23
12. Johnson TR, Krauss B, Sedlmair M, et al. (2007) Material differentiation by dual energy CT: initial experience. Eur Radiol 17:1510–1517
13. Fletcher JG, Takahashi N, Hartman R, et al. (2009) Dual-energy and dual-source CT: is there a role in the abdomen and pelvis? Radiol Clin North Am 47:41–57
14. Patel BN, Thomas JV, Lockhart ME, Berland LL, Morgan DE (2013) Single-source dual-energy spectral multidetector CT of pancreatic adenocarcinoma: optimization of energy level viewing significantly increases lesion contrast. Clin Radiol 68:148–154
15. Flohr TG, McCollough CH, Bruder H, et al. (2006) First performance evaluation of a dual source CT (DSCT) system. Eur Radiol 16:256–268
16. McNamara MM, Little MD, Alexander LF, et al. (2015) Multireader evaluation of lesion conspicuity in small pancreatic adenocarcinomas: complimentary value of iodine material density and low keV simulated monoenergetic images using multiphasic rapid kVp-switching dual energy CT. Abdom Imaging 40(5):1230–1240
17. Lu DSK, Vedantham S, Krasny RM, et al. (1996) Two phase helical CT for pancreatic tumours: pancreatic versus hepatic phase enhancement of tumour, pancreas and vascular structures. Radiology 199:697–701